Characterizing magneto-plasma parameters in extragalactic jets & lobes

1. Extend Earth-bound laboratory experiments to the most energetic magneto-plasma systems in the universe

2. Some opportunities and roadmaps for the next decade

Philipp P.Kronberg
Los Alamos National Laboratory

Workshop on Plasma Astrophysics
PPPL, Princeton NJ
18-21 January 2010

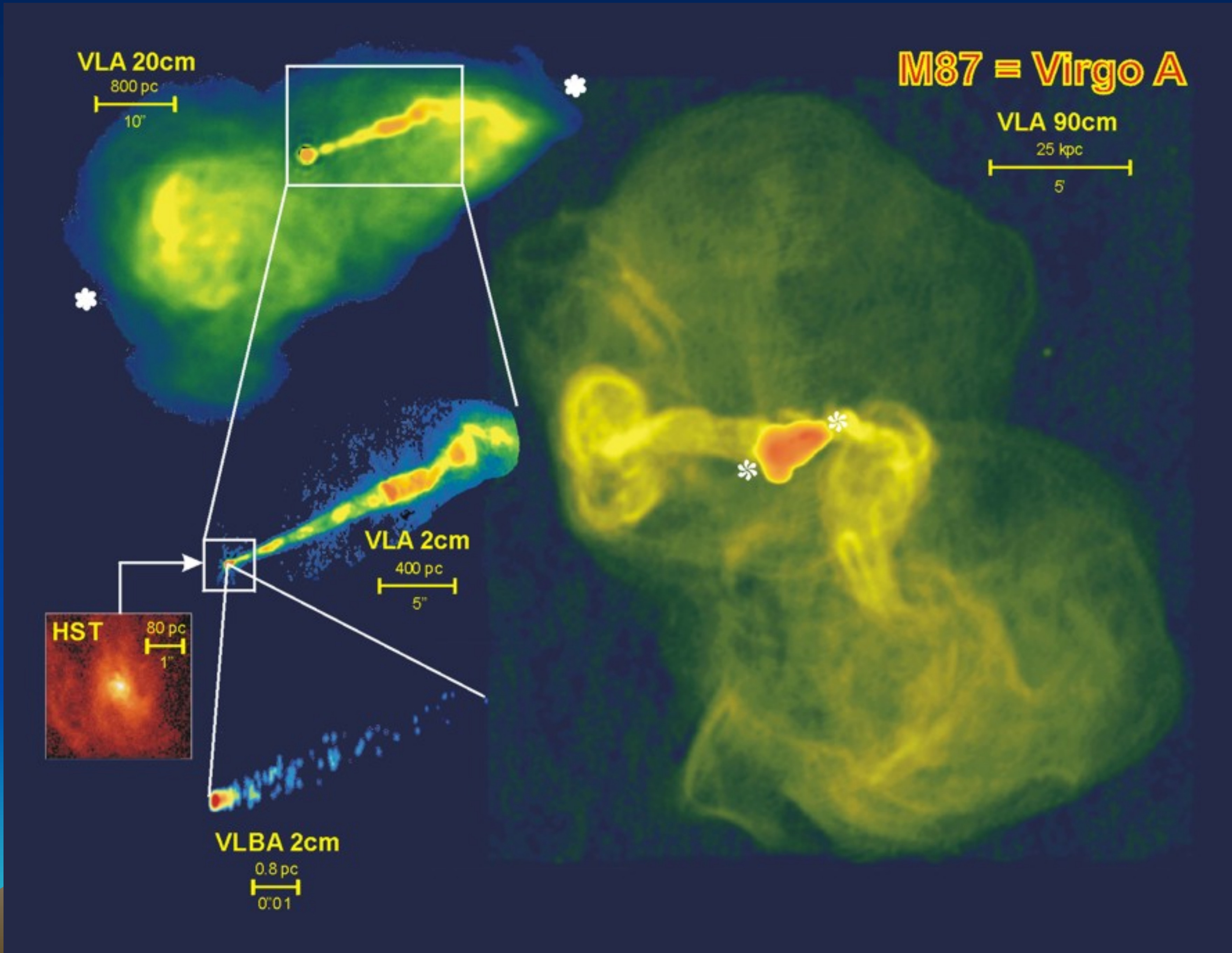

M87 = Virgo A
VLA 20cm
800 pc
10"
VLA 90cm
25 kpc
5'
VLA 2cm
400 pc
5"
HST
80 pc
1"
VLBA 2cm
0.8 pc
0."01

Magneto-plasma jets <u>near</u> the BH-accretion disk

- Some state-of-the-art observations

Sum of 23 VLBA images at 43 GHz

Veritas Collab,

NRAO VLBA M87 Monitoring Team,

H.E.S.S. Collab. & MAGIC Collab., **Science**, **325**, 444, 2009

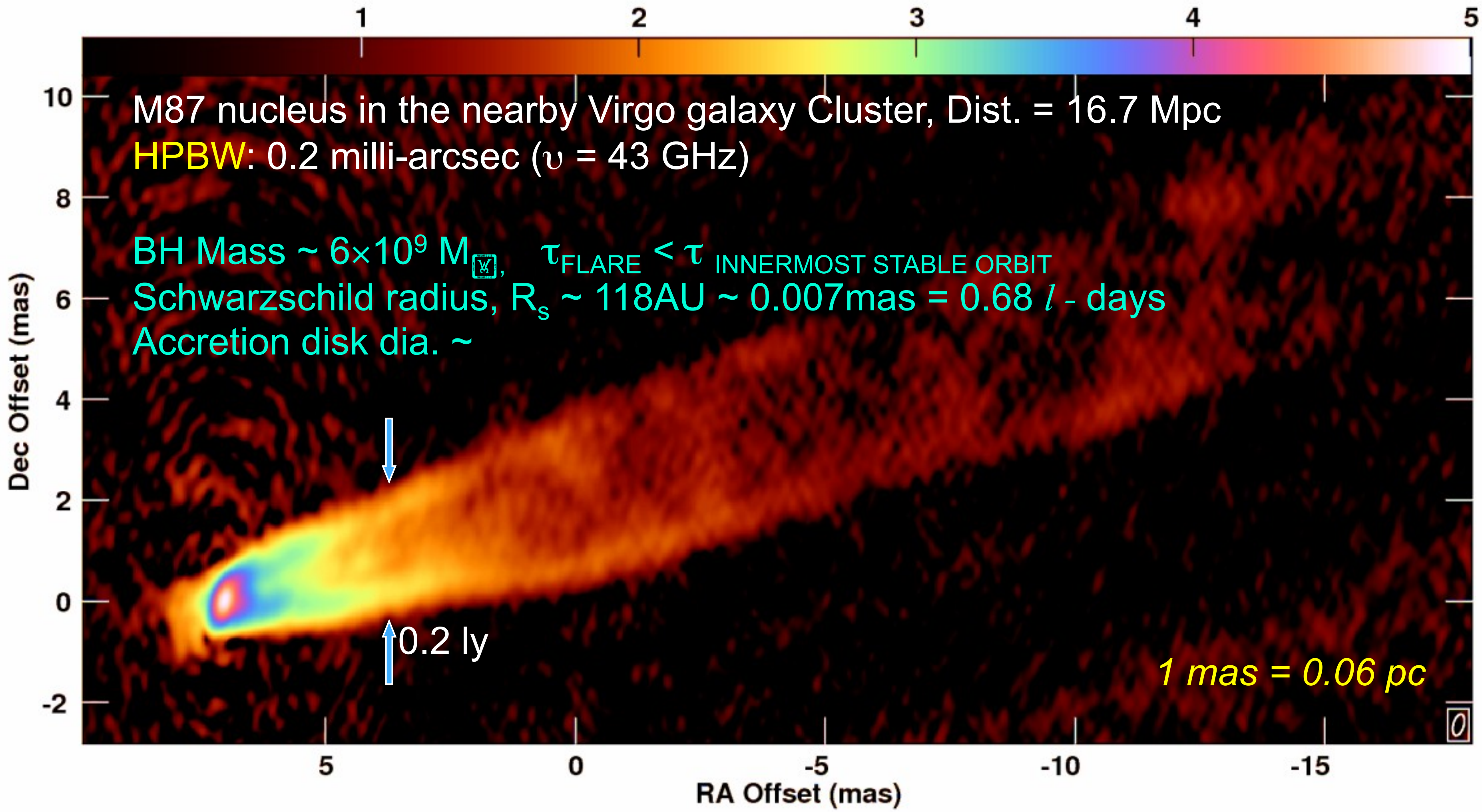

M87 jet 23-frame time sequence
Craig Walker et al. 2008

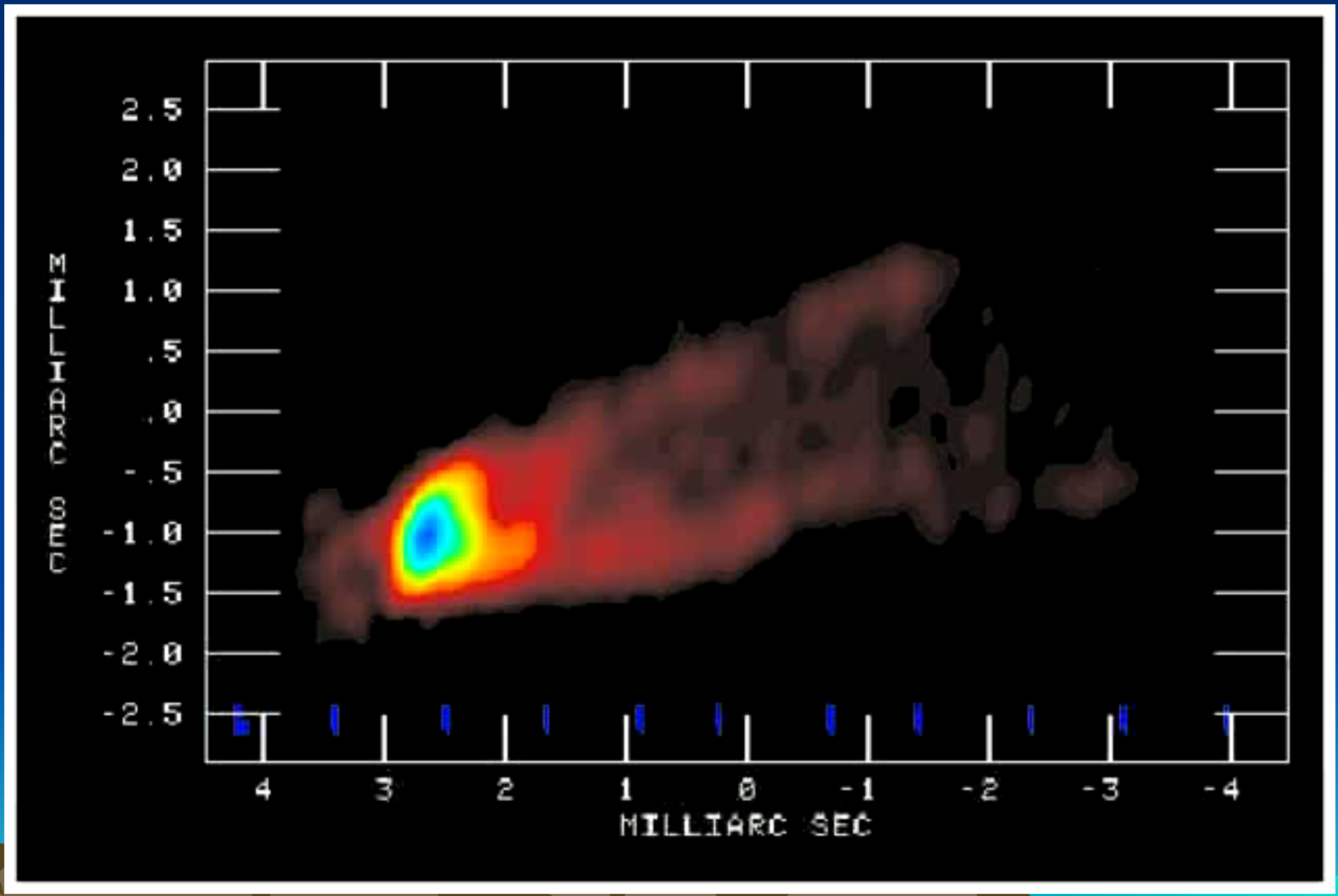

Croke, O'Sullivan & Gabuzda (2009)

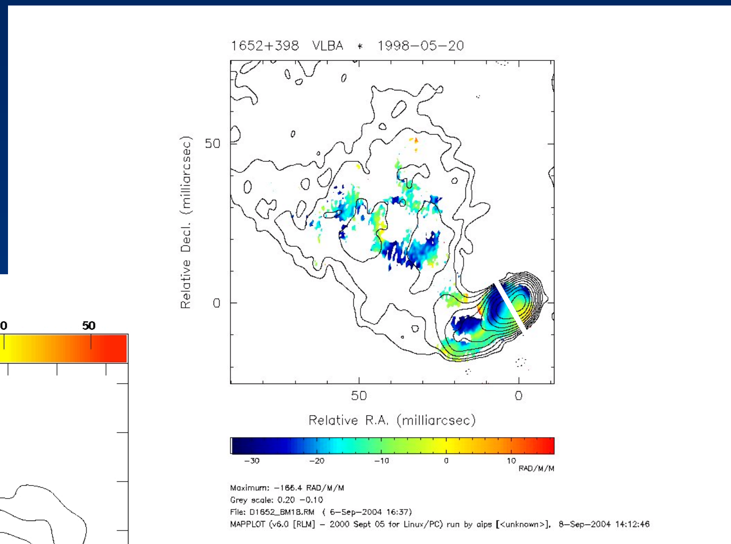

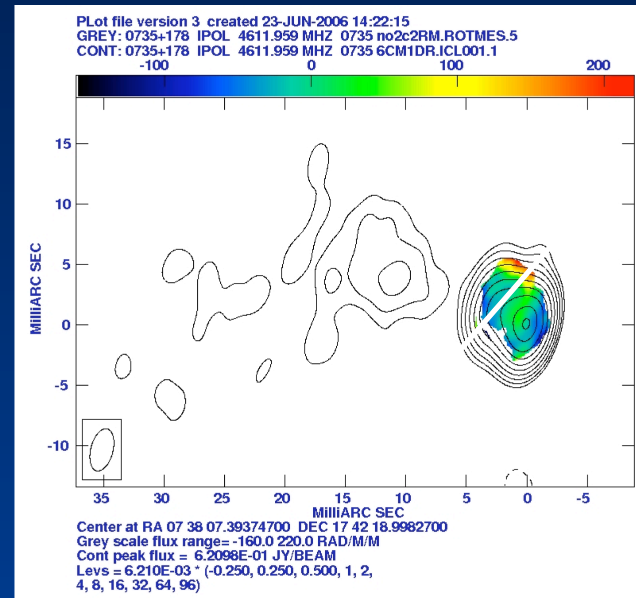

Gabuzda, Vitrishchak, Mahmud & O'Sullivan, MNRAS, 2008

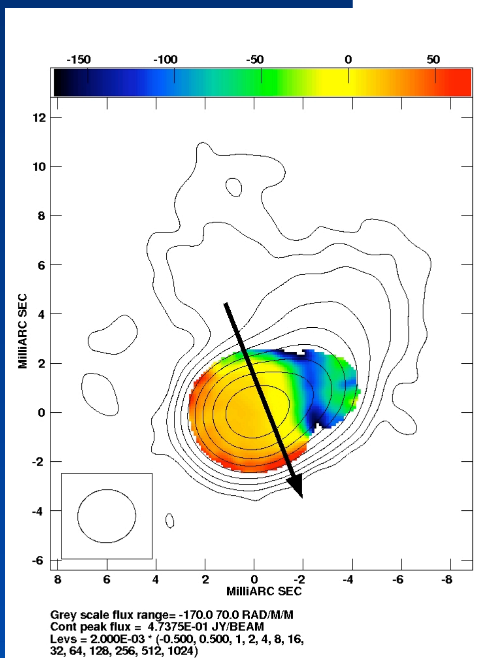

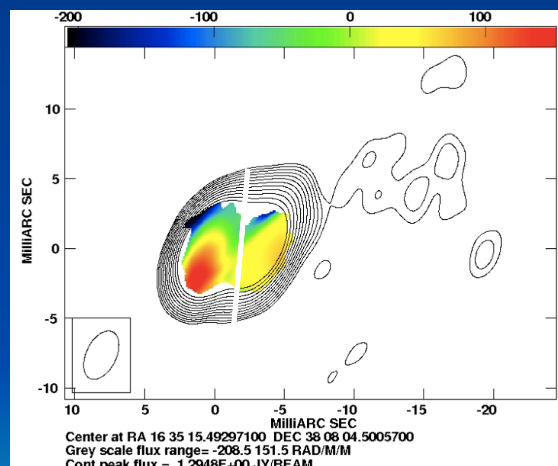

Reichstein & Gabuzda

Mahmud & Gabuzda 2008

Transverse RM gradients have been detected in nearly 30 parsec-scale AGN jets: direct evidence that helical B fields are common in AGN jets

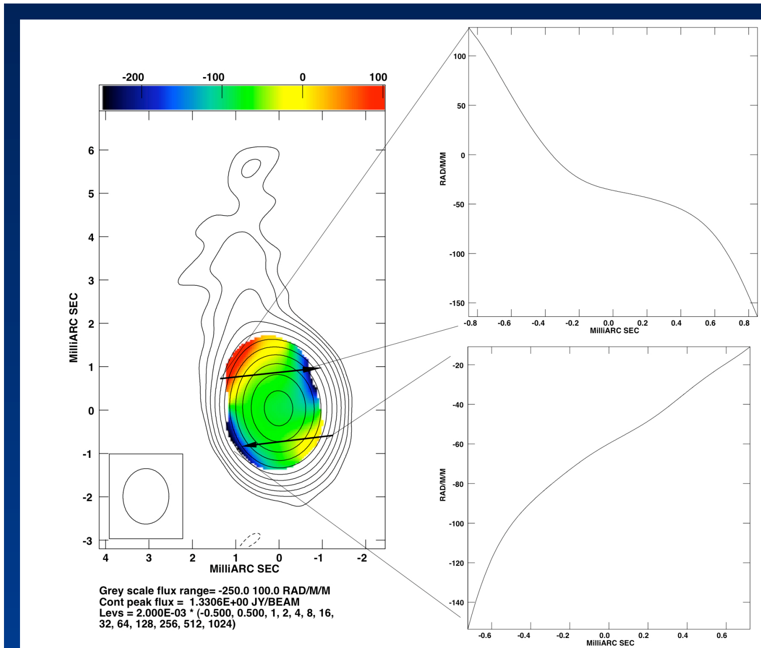

Reversals in the direction of the transverse RM gradient between core region and jet observed in ~ 6 AGN (*Mahmud, Gabuzda & Hallahan* ***MNRAS*** **400,** 2, *2009*)

Mahmud et al.'s interpretation:

May be due to winding up of field that emerges in inner accretion disk and closes in outer disk.

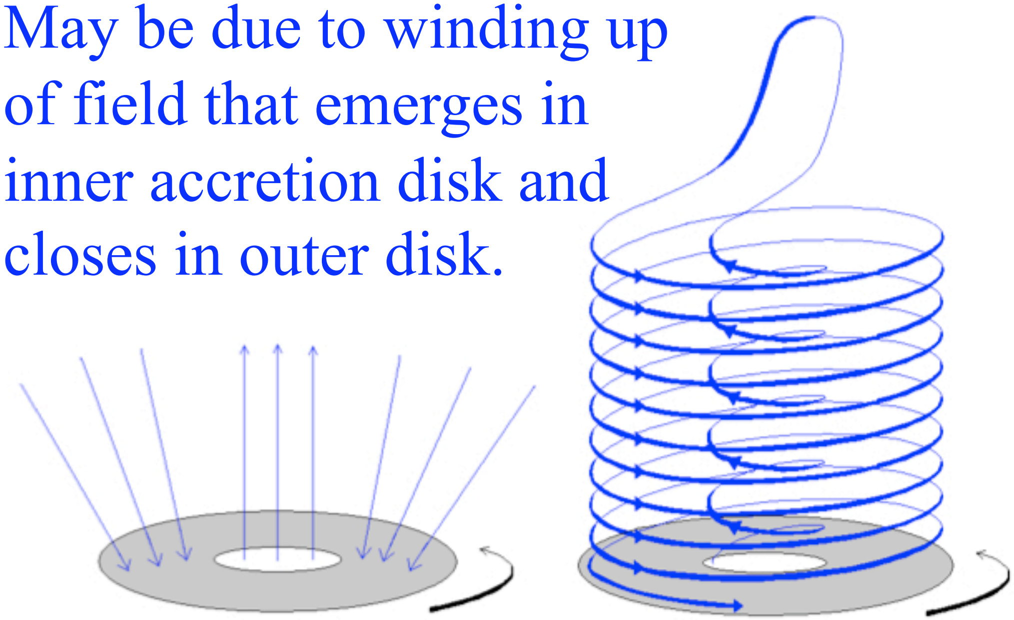

Forms "nested helical field" structure: inner/ outer helical B field dominates total RM in core region/jet.

Evidence that jet B field closes in the outer accretion disk

"Los Alamos" suite of models for BH infall energy release into a Poynting flux-dominated jet

Colgate, Li, Pariev, 2001
Phys. of Plasmas 8, 2425

Li, Colgate, Wendroff, Liska
2001 ApJ 551, 874

Accretion disk dynamo
(S.A. Colgate)

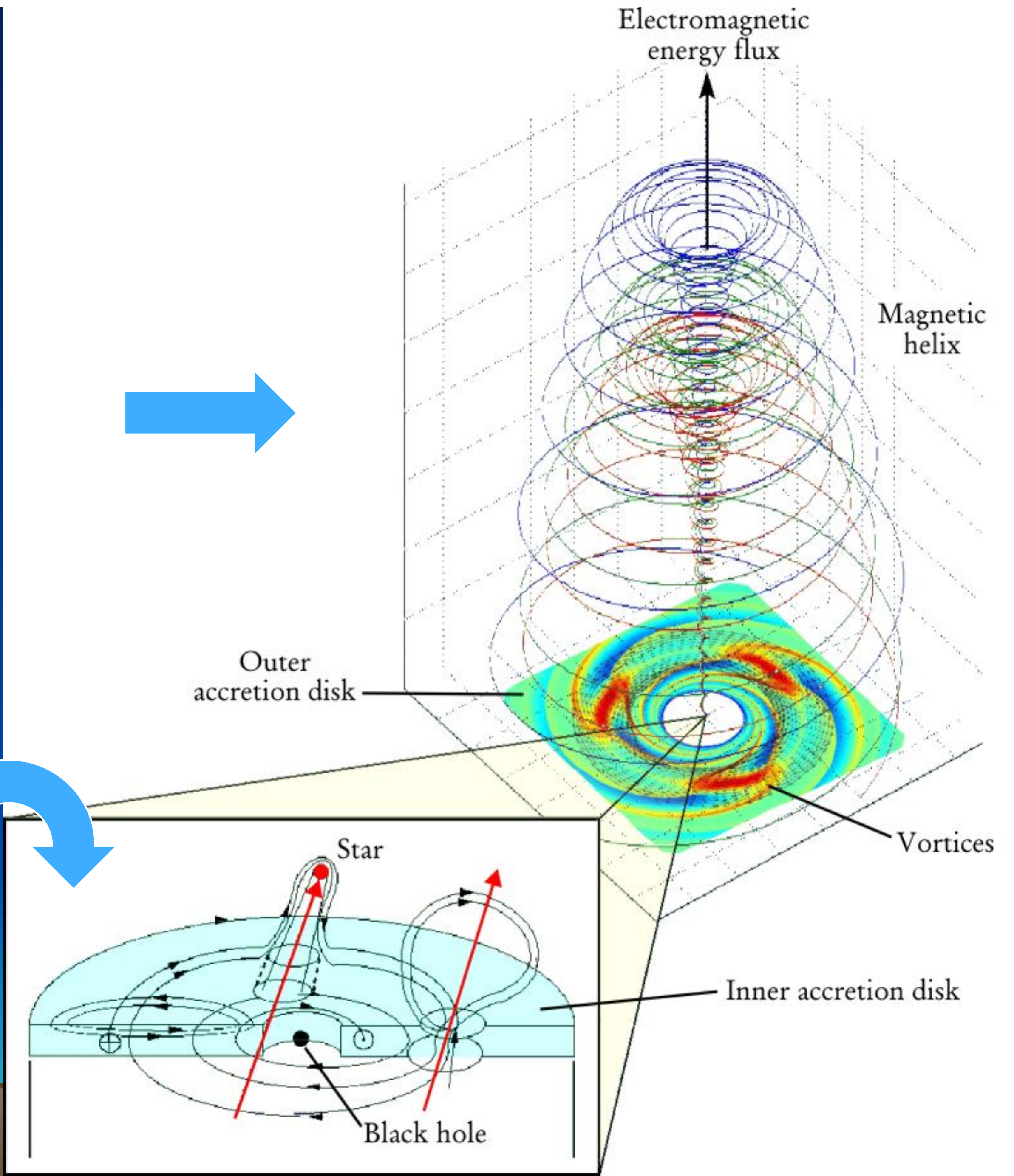

The Poynting-Robertson battery
(Contopoulos, Kazanas, Christodoulou)

- Charges rotating with accretion disk absorb photons from central region of AGN

- Photons are re-radiated isotropically in rest frame of the charges, radiation is "beamed" in direction of their motion in observer's frame

- Thus, they feel a reaction force:

$$F_{\text{P-R}} = -\frac{L\sigma_{\text{T}}}{4\pi r^2 c}\frac{v_\phi}{c}$$

- Force on e^- >> force on p^+ ($\sigma_{\text{T}} \propto m^{-2}$)

⇒Causes electric current in direction of rotation, which produces axial B field

Resulting axial B field is "wound up" — azimuthal B-fields for inner and outer helices have specific directions relative to rotation.

Transverse RM gradient from inner helical field is always CW relative to jet base, RM gradient from outer helical field is always CCW, independent of direction of disk rotation:

Contopoulos et al. ApJ.,702, L148, (2009)

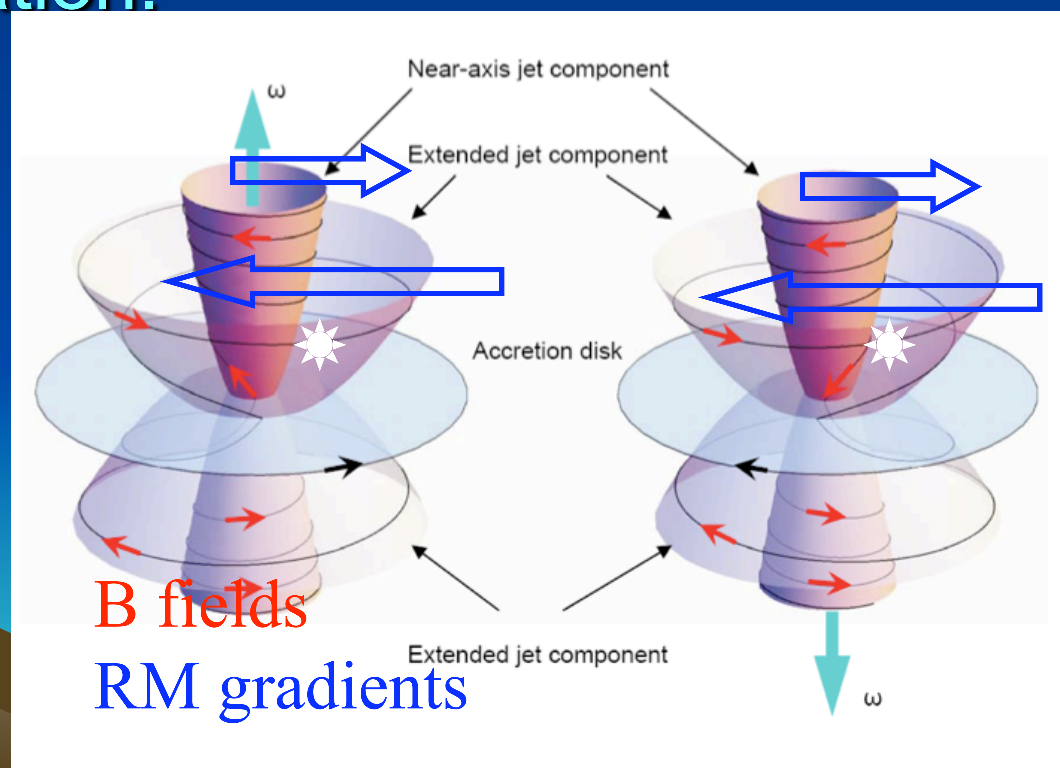

M87
on VLBI/parsec scales

Left: Eqiuipartition-derived

B field falls off as r^{-1}. B at 1 pc is ~ 0.3 G.

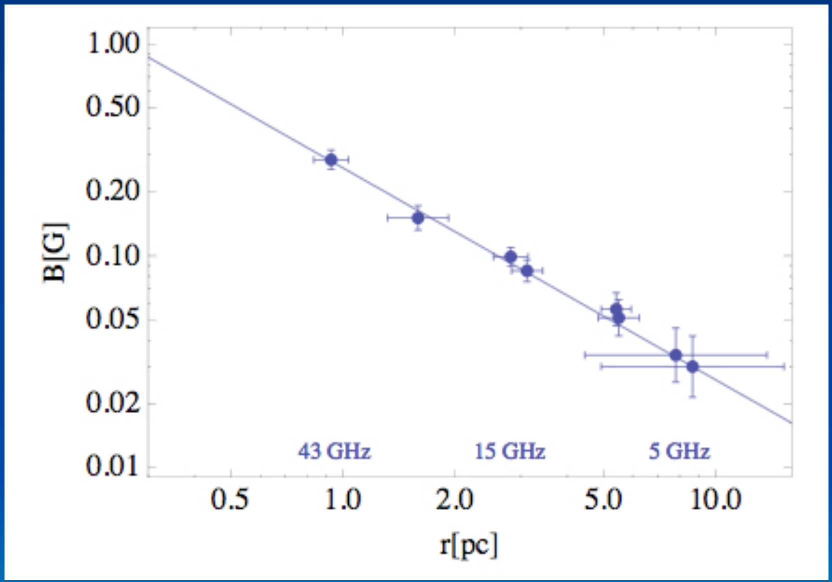

Right: B fields extrapolated to r_g and $10r_g$ agree with expectation for a magnetically powered jet

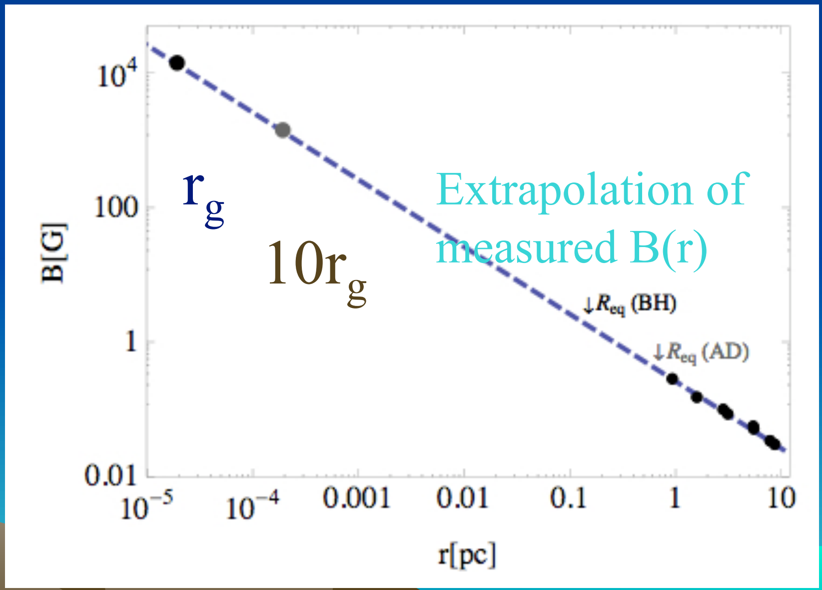

O'Sullivan, S. P., & Gabuzda, D.C. MNRAS 400, 26, 2009

Now to kpc+-scale jets

Knots and Hotspots of 3C303 (z=0.141)

Radio (VLA) and X-Ray (CHANDRA)

P. Kronberg, Can.J. Phys ***64,*** *449, 1986*

P. Leahy & R. Perley, Astr. J. ***102,*** *537, 1991*

J. Kataoka, P. Edwards, M. Georganopoulos, F. Takahara, & S. Wagner A&A ***399,*** *91, 2003*

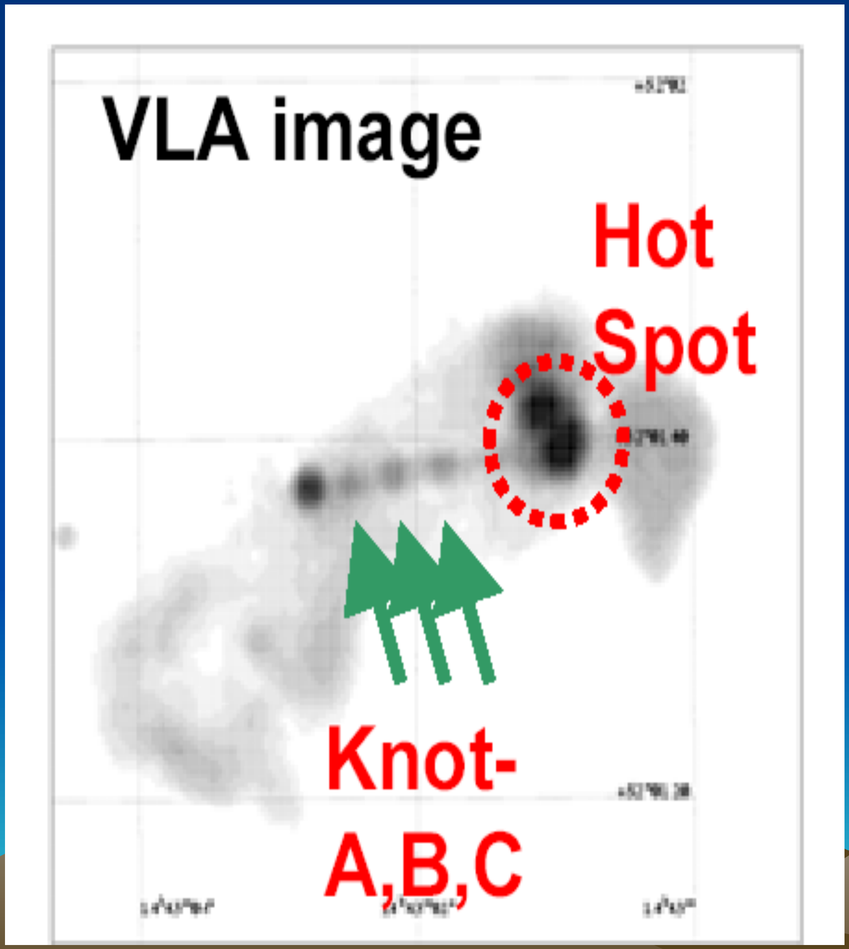

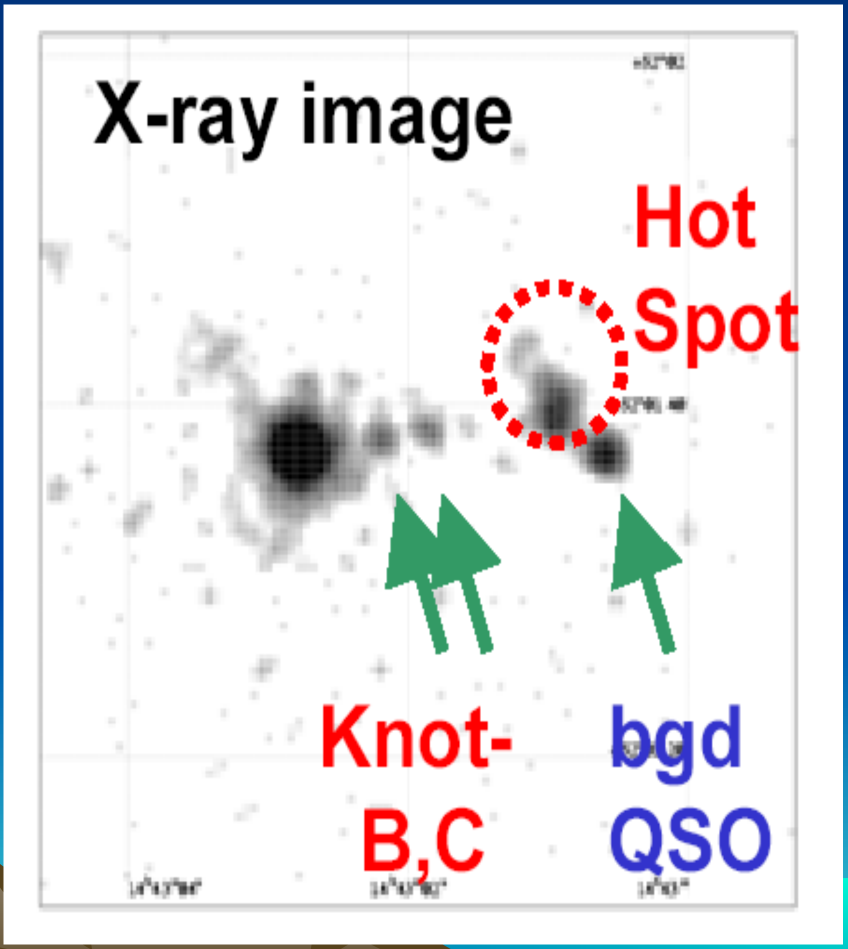

Let's create a "laboratory" to deduce (BH-powered) 3C303's plasma parameters:

- from multi-frequency VLA radio, and Chandra X-ray images

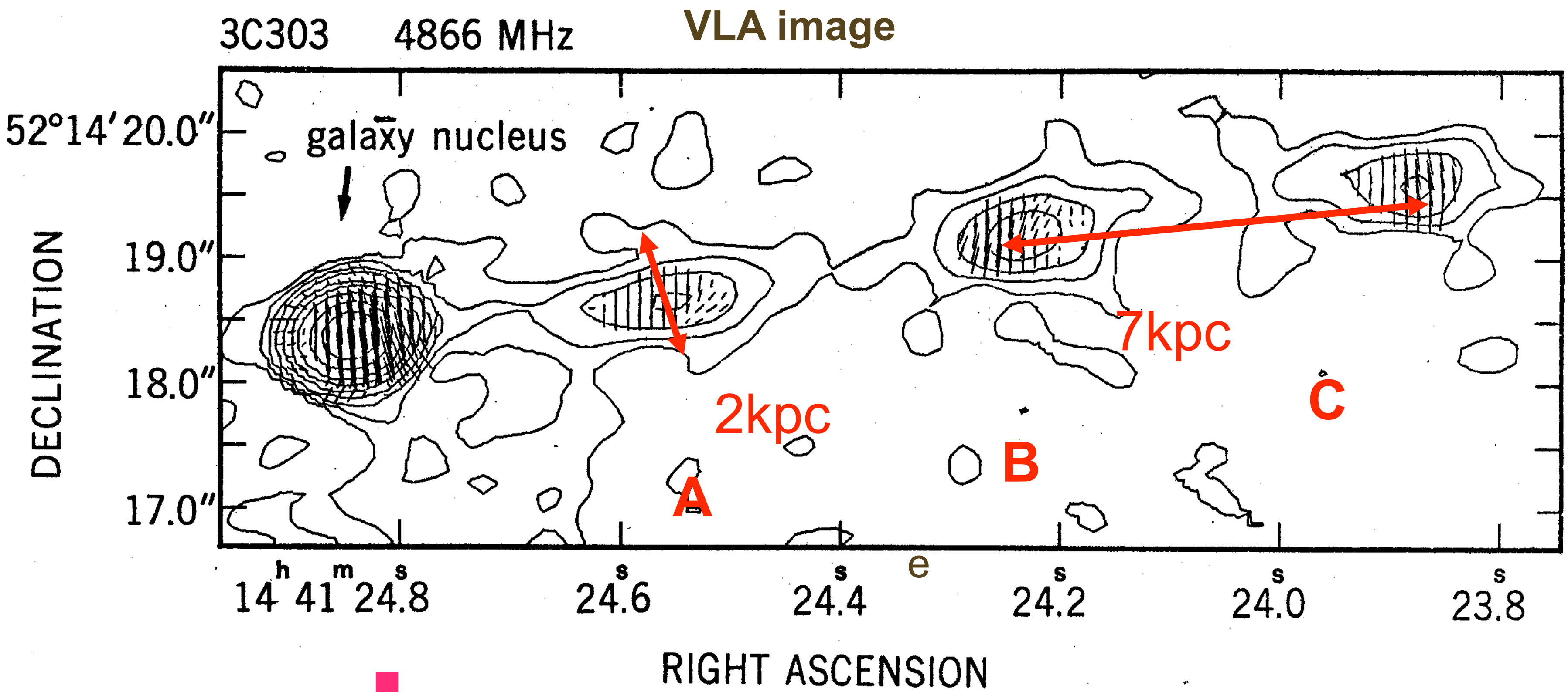

Compare scales!

21cm radio luminosity of the M87 jet = 0.12Jyx4πD^2 = 4.87x10^{31} erg sec^{-1} Hz^{-1}

3C303 knot lengths ≈ 25× those in M87!

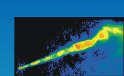

Entire M87 jet on the scale of 3C303!!

M87 Knot volumes are ~ 12,000 times smaller than those in 3C303!

SMBH-powered jets are very scale-independent systems!

Plasma Diagnostics of the 3C303 jet

Lapenta & Kronberg ApJ 625, 37-50, 2005

(1) $<$(Total energy flow rate)$>$ $\equiv E^T_{min}/\tau$ = **2.8x10^{43}** τ_7^{-1} erg/s

(2) Total radio → X-ray luminosity of the jet ≡ **1.7 x 10^{42}** erg s^{-1}

$\frac{(2)}{(1)}$ ⇒ Radiative dissipation from the jet ≈10% of energy flow rate along jet!

(3) Measure knots' synchrotron luminosity & size (D_{knot}) ⇒ $B^{knot}_{int}=10^{-3}$G

(4) From the Faraday rotation images of the knots (**RM** ∝ n_{th} × B^{knot}_{int} × D_{knot})

⇒ **n_{th} in knots (*upper limit* for 3C303) ⇒ n_{th} ⇒ 1.4×10^{-5} cm^{-3}**

(3) & (4) ⇒ lower limit to V_A within knots : V_A^{knot} ∝ B^{knot}_{int} / $(n_{th})^{1/2}$

RESULT: V_A^{knot} ≈1.9*c*. i.e. close to *c*, or V_A^{rel}

Plasma parameters in the 3C303 jet

- Given *B* and n_{th} measured in the 3C303 jet, (scaling to $T=10^8$K)
- Plasma β = $\frac{nkT}{\left\{ B^2 / 8\pi \right\}} \approx 10^{-5}\, T_8$, confirms very little thermal plasma
- $|B|$ ~ 3 mG in the synch. radiating jet knots (cocoons), over ~ 1kpc
- *Consistent with a magnetically confined, Poynting flux driven jet.*

Lapenta & Kronberg ApJ 2005

How to estimate the jet current? --

Combine the above measurements with Faraday rotation information

we need:

1. Faraday RM image of the jet from images at ν_1, ν_2 …etc., at a common angular resolution

2. Background sky RM's to establish the zero- level of RM, then subtract it from the RM's in the source image

Faraday Rotation Image of 3C303

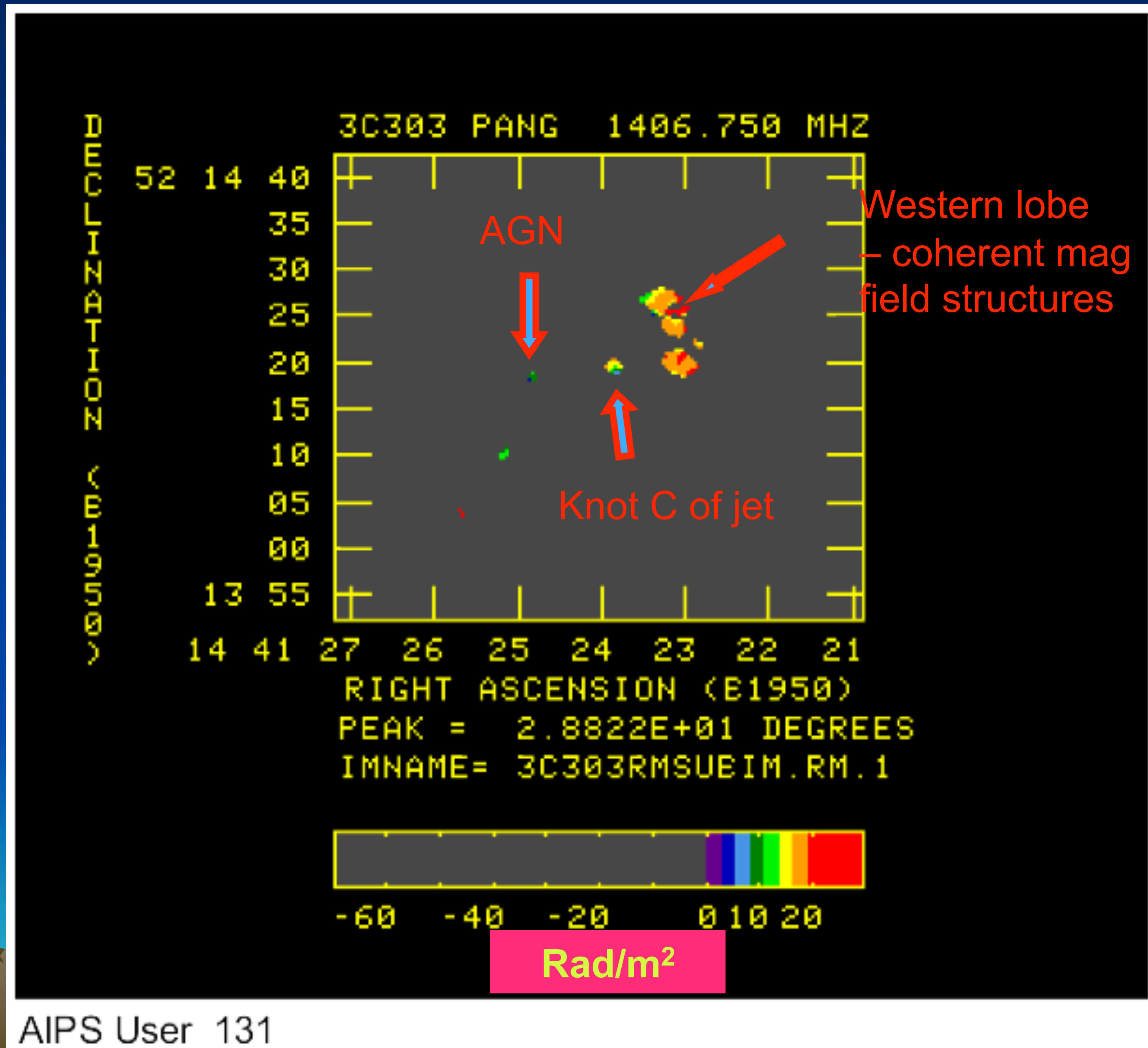

- the RM image of 3C303 enables a measurement of the ∇RM (radians/m^{-2}/m) over a knot.
- ∇RM is perpendicular to jet at knot "C", !
- Also, line of sight B (RM) reverses sign on the jet axis.
  (Recall that |B| (≅ 1mG) is estimated from measured synchrotron emissivity

CONCLUSIONS:

- 3C303 jet behaves as a galaxy-scale, current-carrying "wire"
- Current deduced : I = 7.5 x 10^{17} (B^{G}_{-3}) [r= 500pc] ampères
- I is directed AWAY from the galaxy AGN nucleus in this knot
- Intrinsic knot polarization consistent with low-ϕ helical field

Reported in

H. Ji, P.P. Kronberg, S.C. Prager, D. Uzdensky, *Physics of Plasmas* **15**, *058302-8, 2008*

and

G. Lapenta & P.P. Kronberg *ApJ* **625**, *37, 2005*

3C303 results lead to other simple electrodynamic calculations

- B_r (~1 mG at r = 500pc) follows the same 1/r relation as the recent VLBI estimates at 1 [illegible] r [illegible] 10pc !
- The l.h. side of the jet power source feeds out $2.8{\times}10^{36}$ watts of e.m. power
- 3C303's jet current is $7.5{\times}10^{17}$ amps
- The BH system ``sees'' an impedance:

  $Z = P/I^2 = 2.8 \times 10^{36} / (7.5{\times}10^{17})^2 \approx 3\, I_{18}^{-2}$ ohms

Within current uncertainties, near the impedance of free space!

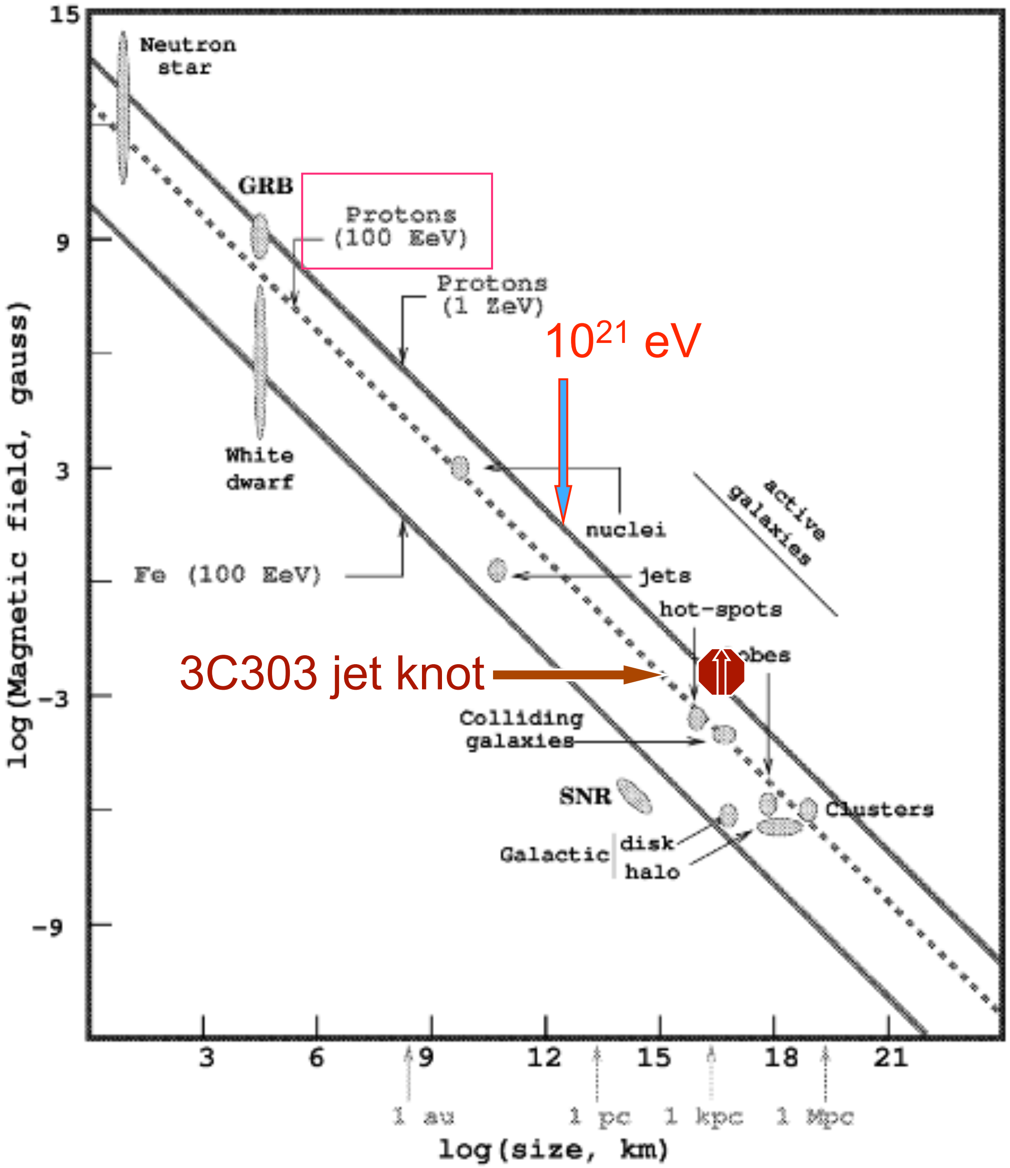

UHECR acceleration in the 3C303 jet?

B·L ("Hillas") plot
(*A.M. Hillas AnnRevAstAp 1984*)

knot parameters make the jet a potential acceleration site for CR nuclei up to ~ 10^{21} eV

Opportunities

Future instrumental directions and opportunities

Essentials

- Need angular resolution 6x to 50x better , with optimum sensitivity
- Need Multi-frequency polarimetry & good frequency coverage
- ALL OF THESE ARE POTENTIALLY IN HAND

PARSEC SCALE jet launching regions

-- [illegible] 6 x more better VLBI resolution is within reach
-- increase observing frequency to 90GHz (2.6mm) and 120GHz (1.8mm)
-- include more, large radio telescopes, longer baselines
--extend bandwidths
--measure and calibrate all Stokes' parameters

- **KPC SCALE jets: (e.g. 3C303)**

-- [illegible]15x more resolution needed (35km (EVLA) → 500km)
-- (1) wide freq coverage at (2) much greater sensitivity
and (3) longer baselines
-- (1) and (2) are newly implemented (new EVLA WIDAR correlator)
-- (3) possible with the proposed EVLA2, (``The New Mexico Array") – 6 – 10 more EVLA dishes covering several hundred km, Cost: ~ $200M
-- but the EVLA2 proposal was recently shelved or withdrawn
-- alternative could be EVLA + e-Merlin (UK/European interferometer)
-- For Faraday RM imaging, need ν [illegible] 1 GHz
-- insufficient resolution is not solved by simply going to higher frequencies!!

Magnetic stability of the lobes

Near future instrumental capabilities are in good shape

- Enhanced VLA,
- Upgraded Arecibo telescope,
- LOFAR
- X-ray telescopes
- TeV γ-ray telescopes,

S.Diehl, H. Li, C.Fryer, D. Rafferty 2008 ApJ

Hydra cluster X-ray image:

Wise, M.W., McNamara, B.R., Nulsen, P.E.J, Houck, J.C., & David, L.P. ApJ ***659****, 1153, 2007*

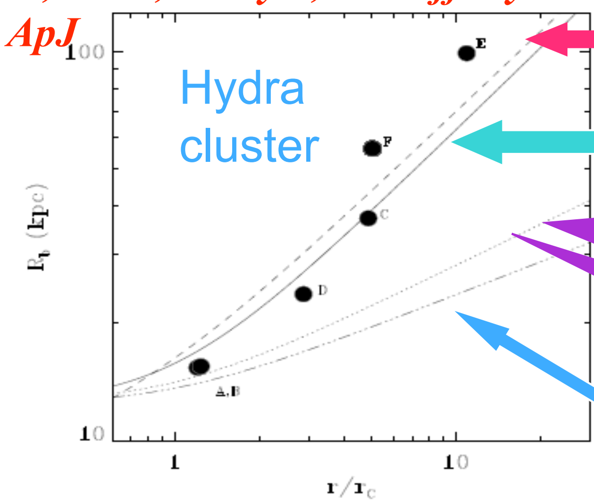

FIG. 6.— *Left:* The multi-cavity system in Hydra A, reproduced from Wise et al. (2007) with permission from the authors. The black area is excess X-ray emission left-over after an elliptical surface brightness model has been subtracted. *Right:* Data Points: Bubble sizes for Hydra A as a function of distance to the center, taken from Wise et al. (2007); Lines show predictions from the AD53 (triple-dot dashed line), AD43 (dotted line), FML (also dotted line), CIH (dashed line), as well as the CDJ model (solid line). The cavity labels are the same in both plots.

CIH continuous injection hydrodynamic model - - -

CDJ current-dominated MHD jet model ———

FML Bubbles contain frozen-in mag. loops

AD Γ=5/3, **AD Γ=4/3** Adiabatically expanding hydrodynamic models

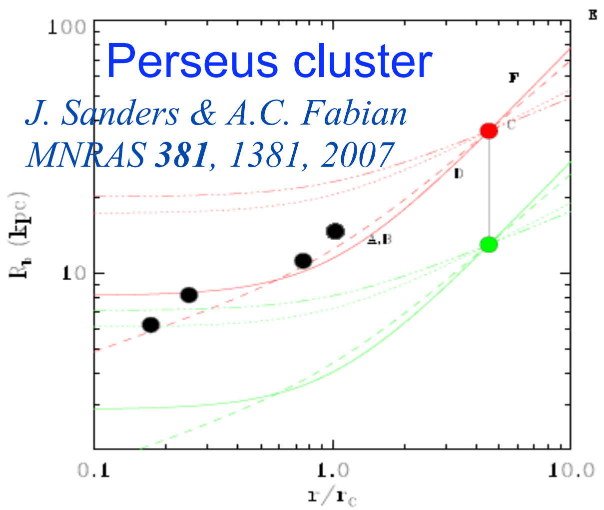

FIG. 7.— Bubble sizes for Perseus as a function of distance to the center. Lines as in Figure 6. The red data point shows the upper limit for the new bubble size estimate, the green data shows a lower limit. The correct answer will likely lie somewhere in between these two extremes.

limits to the true location of the bubbles. This will not only affect the radii themselves, but also the point at which other quantities are evaluated at, like density, temperature and pressure. In general the temperature rises outward in these systems, thus the temperature at the location of the bubble is likely to be systematically underestimated. The density and ambient pressure on the other hand will always be overestimated. This also means that any rise times derived from using the projected radius rather than the true distance to the center will result in estimates for the rise times that are systematically too low. We also note that the smaller the observed radius is, the higher the probability that it is due to an effect caused by projection.

But there are more subtle effects that projection has on our data. As we do not have an automated tool to detect bubbles, one has to rely on human experience in finding and identifying these systems. This task is much more difficult, if the cavities overlap with the bright cluster center or the bubble on the opposite side of the cluster. In fact, our sample does not contain *any* cavity system in which the bubble size exceeds the projected distance to the center, the slope of which is shown by the black solid line in Figure 8, even though this is statistically very improbable. This suggests that our sample is affected by what we will refer to as a "geometric" selection effect, introduced by our manual detection process.

Effects of Sig/Noise and projection effects; *Enßlin & Heinz A&A* ***384****, L27, 2002*

See Hui Li's presentation

The largest ("giant") radio galaxies are
CALIBRATORS OF BH MAGNETIC ENERGY OUTPUT

Accumulated energy output is magnetic + CR ($\approx 10^{61}$ ergs)
On an intergalactic scale it is "captured" within a few Mpc,
(in contrast to the photon energy)

2147+816 giant radio galaxy

Analysis of ≈ 70 GRG images
Kronberg, Dufon, Li, Colgate
ApJ 2001

z=0.146

2.6 Mpc

8 FRII-like GRG's, w. detailed,
multi-λ obs. & analysis
Kronberg, Colgate, Li, Dufton ApJL 2004

- Willis & Strom, 1978,80
- Kronberg, Wielebinski & Graham.1986,
- Mack *et al.* A&A 329, 431, 1998
- Schoenmakers *et al.* 1998,2000
- Subrahmanian *et al*. 1996
- Feretti *et al* 1999
- Lara *et al*. 2000
- Palma *et al*. 2000

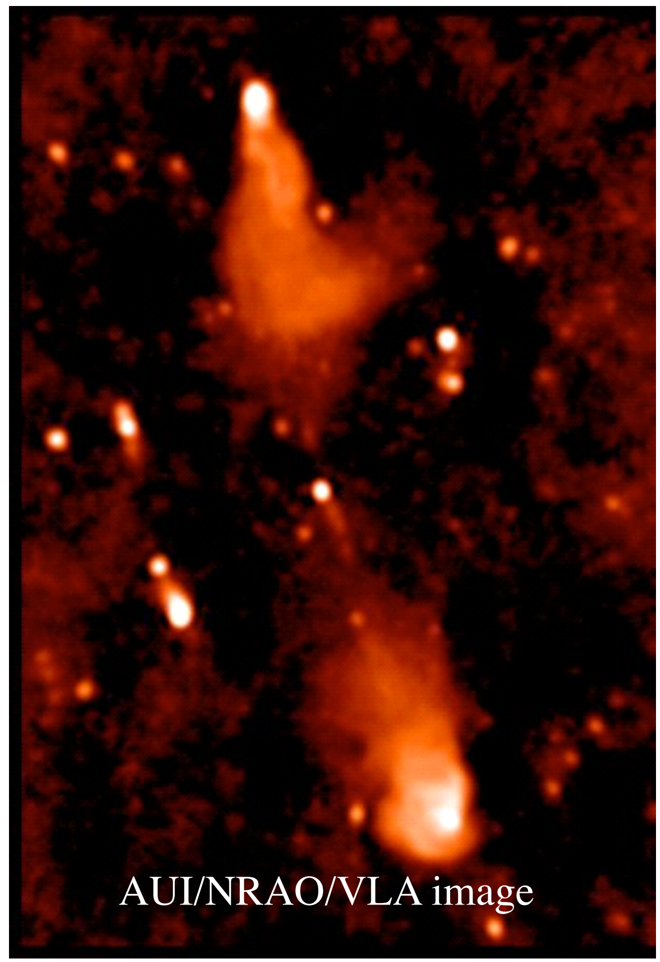

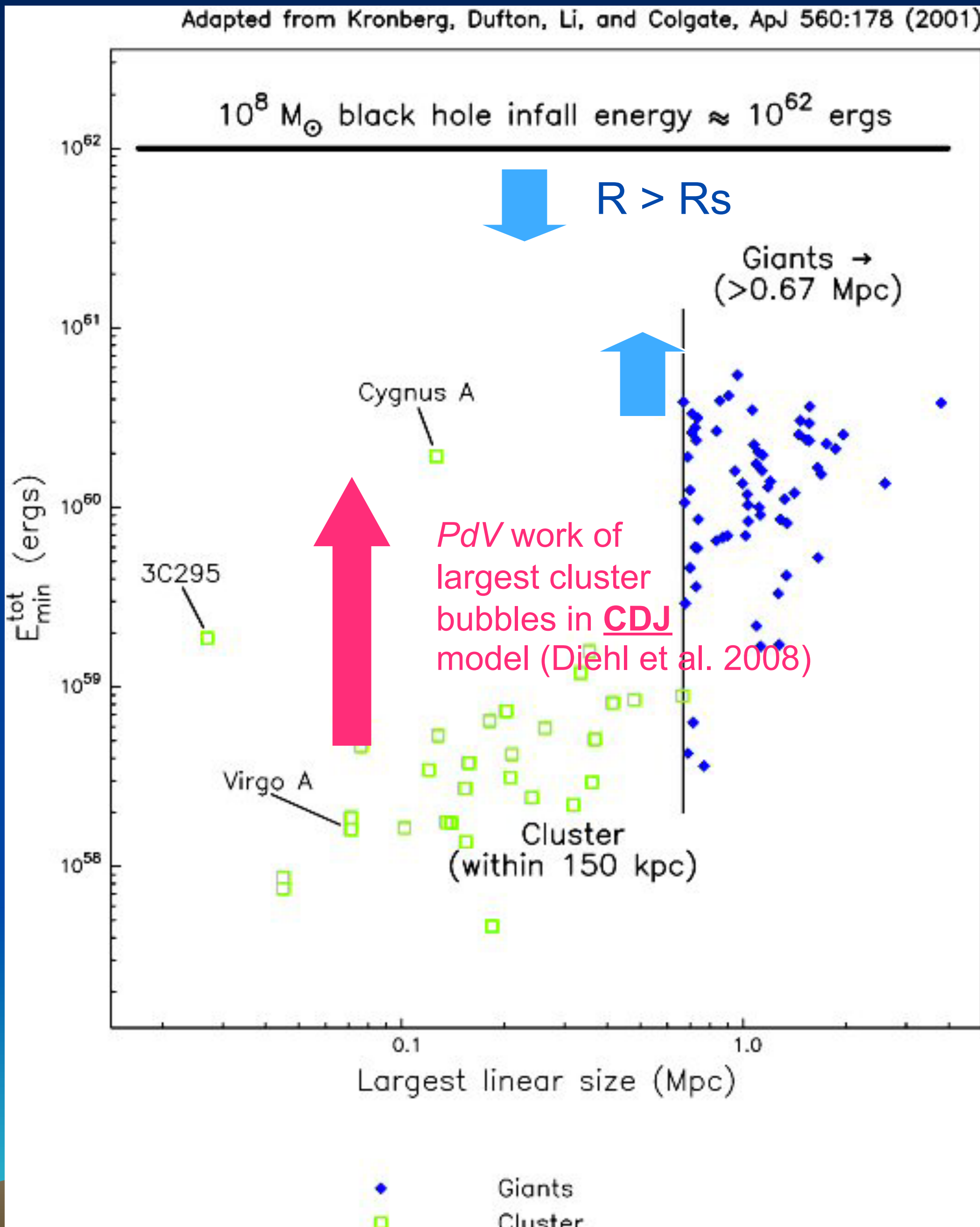

$=M_{BH}c^2$

Mind the gap!!

Accumulated energy
($B^2/8\pi$ + ε_{CR}) x (volume)
from ``mature'' BH-powered
radio source lobes

GRG's
capture the highest fraction
of the magnetic energy
released to the IGM

Kronberg, Dufton, Li, & Colgate,
*ApJ **560**, 178, 2001*

The End

P.P. Kronberg LANL